

Identification of Minority Ion-Cyclotron Emission during Radio Frequency Heating in the JET Tokamak

G. A. Cottrell

JET Joint Undertaking, Abingdon, Oxon OX14 3EA, United Kingdom

(Received 2 September 1999)

First measurements and identification of minority ion-cyclotron emission (MICE) during ICRF (H)D minority heating in the JET tokamak are presented. An inner wall radiofrequency (rf) probe shows the new single MICE spectral line, down-shifted from the heating frequency and appearing ~ 400 ms after the ICRH switch-on. The line is narrow ($\Delta\omega/\omega \approx 0.04$), characterized by the ion-cyclotron frequency of minority protons in the outer-edge midplane plasma and is observed irrespective of whether single or multifrequency ICRH is applied. The observations are consistent with the classical evolution and population of the plasma edge with ~ 3 MeV ICRH protons on orbits near the outboard limiters. Particle loss and energy filtering contribute to a local non-Maxwellian energetic ion distribution, which is susceptible to ion-cyclotron instability.

PACS numbers: 52.25.Sw, 52.35.Qz, 52.50.Gj, 52.55.Pi

Information about the population of superthermal ions in a tokamak can be obtained by making measurements of ion-cyclotron emission (ICE). Previous ICE measurements [1–4] on the JET tokamak (major radius $R_0 = 2.96$ m, minor radius $a = 0.9$ m, plasma current $I_p \leq 7$ MA, and toroidal magnetic field $B_T \leq 3.8$ T) used a low field side ion-cyclotron range of frequency (ICRF) heating antenna to detect plasma radiation up to 200 MHz. The rf spectra of both pure D-D and mixed D-T discharges contain narrow cyclotron emission lines, with equal spacing proportional to B_T . The intensity is larger than the thermal ion blackbody level, indicating that ICE is driven by energetic ions. The detected emission comes from a localized region ($\Delta R \leq 0.2$ m), and the emission lines coincide ($\omega = l\Omega_D = l\Omega_\alpha$) with harmonics, l , of the D and fusion α -particle gyrofrequencies in the outer midplane edge [3]. The intensity of the superthermal ICE in JET is proportional to the total fusion reactivity over a range of six decades of signal intensity [4], connecting it with the birth of 3 MeV D-D fusion protons and 3.5 MeV D-T fusion α particles which are born mainly in the plasma center. A fraction of these particles are deeply trapped in the tokamak magnetic field and make sufficiently large drift orbit radial excursions enabling them to intersect the edge plasma where they are both super-Alfvénic and the ICE is observed. ICE has also been observed on other tokamaks, notably on TFTR where emission from both energetic fusion product and neutral beam injected ions has been observed; these results are compared with the ICE seen in JET and several other tokamaks in Ref. [5]. In this paper, we shall refer to fusion product driven ICE as FP-ICE to distinguish it from minority ion driven ICE. The potential of FP-ICE has already been discussed as an α -particle diagnostic for D-T experiments [4,6,7]. With minority ion-cyclotron emission (MICE), ion-cyclotron-resonance heating (ICRH) can be used to inject into the tokamak edge a sufficiently large population of energetic ions to stimulate ICE and so give the advantage of allow-

ing ICE physics to be studied experimentally without the use of D-T fuel.

Minority protons heated by centrally resonant ICRF in JET form an energetic tail. Ions gain energy perpendicular to the magnetic field and can enlarge their drift orbital widths sufficiently to enable them to intersect the edge plasma [8] where they mimic certain aspects of fusion protons. In steady state, the minority ion energy distribution is characterized by an asymptotic perpendicular tail temperature [9], $T_\perp \approx \rho_{\text{rf}}\tau_s/2n_m$, where, for JET ICRH experiments with low minority number density, $n_m = 2.5 \times 10^{17} \text{ m}^{-3}$, the rf power density coupled to the minority ions is $\rho_{\text{rf}} = 0.5 \text{ MW m}^{-3}$, the central number density of electrons is $n_{e0} = 2.5 \times 10^{19} \text{ m}^{-3}$, and the classical ion-electron momentum slowing-down time is $\tau_s = 0.3$ s. The average energy of minority protons in the tail is $\cong 1.5$ MeV, and a fraction of the tail occupies an energy range similar to the 3 MeV D-D fusion protons, responsible for FP-ICE. However, at high enough energies, particles suffer direct losses by striking the outboard limiters. This effect could be simulated by increasing the energy of the low field side resonance ICRH particle orbit shown in Fig. 1 from 3 to 3.4 MeV. The confined particles which just graze the limiter surfaces through the scrape-off plasma are super-Alfvénic: the ratio $v/v_A \cong 1.3$, where v is the local particle velocity, and v_A is the edge Alfvén velocity. Out of the ensemble of confined tail minority ions, only particles with the highest energies can intercept the outer midplane edge plasma. This is because the width of a large D-shaped orbit, such as the one shown in Fig. 1, is proportional to the cube root of the particle energy [10]. Minority ions making large radial excursions into the edge plasma are therefore selected by the natural energy filter of the tokamak magnetic field and contribute, locally, to a “bump-on-tail” velocity distribution. These rf minority ions therefore possess a number of the key physical attributes which are important theoretically in the generation of superthermal

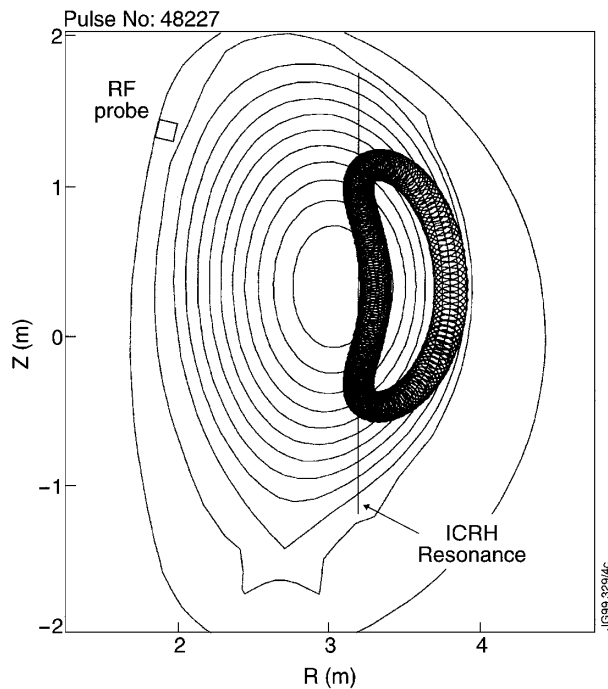


FIG. 1. Poloidal cross-section geometry of the JET tokamak showing the flux contours of a typical X-point discharge (shot No. 48227 at time 4 s) with ICRH. The diagnostic rf probe antenna is shown as well as the D-shaped orbit of an ICRH 3 MeV minority proton.

FP-ICE via the magneto-acoustic instability [6,7]. They are therefore a candidate species to convert their free energy into superthermal ICE by a similar mechanism.

To search for this emission, new rf observations have been made using a high-frequency loop antenna mounted on the upper inner wall of the JET vacuum vessel (Fig. 1). The antenna is connected to a spectrum analyzer used in either scanning or in fixed frequency mode. The advantage of using a separate diagnostic rf antenna and not one of the main JET ICRH antennas is to enable ICE measurements to be made during high-power ICRH experiments. This is the reason why MICE has not been observed in JET until now. The measurements were made during experiments with near-central ICRH in the (H)D regime.

rf spectra of a $B_T(0) = 2.58$ T, $I_P = 2.58$ MA discharge with nearly single-frequency ICRH are shown in Fig. 2. The coupled rf power was $P_{rf} = 4.7$ MW and the H minority concentration was $n_H/n_e \approx 1\% - 2\%$. The frequency of each of four rf generators was tuned within a narrow bandwidth of 130 kHz of the central frequency, $f_{rf} = 37.3$ MHz. Spectra were measured in the frequency range up to 100 MHz with a bandwidth of 100 kHz. The pre-programmed ICRH power waveform was linearly ramped up from 0.5 MW at time 43.35 s to a near steady value of 4.7 MW at 43.66 s. The spectrum is shown at two times after the ICRH flattop. The earlier spectrum shows emission at f_{rf} and the second harmonic, $2f_{rf}$. The later spectrum shows the additional appearance of the MICE line down-shifted to a frequency of 29.6 MHz. The re-

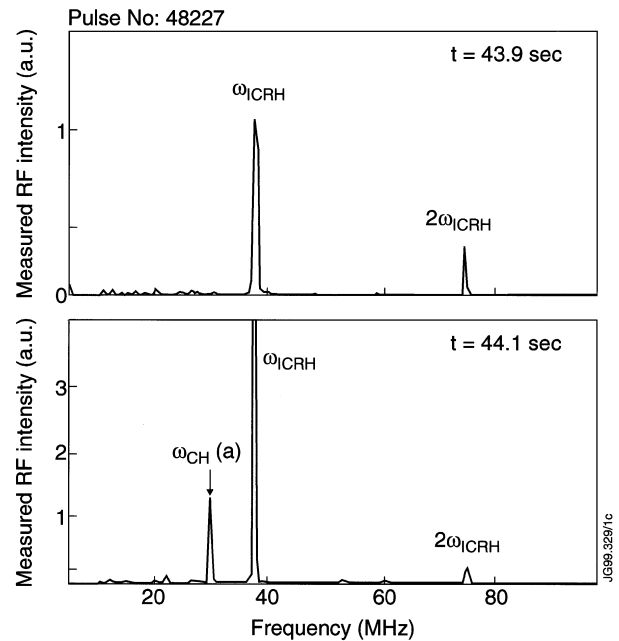


FIG. 2. rf emission spectra measured during single-frequency ICRH. Upper: Spectrum measured 240 ms after ICRH flattop reached; lower: spectrum was measured 440 ms after ICRH flattop reached and showing the MICE line at 29.6 MHz.

solved full width at half maximum (FWHM) of the line is $\Delta f = 1.2$ MHz.

Figure 3 shows the spectrum during multifrequency ICRH with $B_T(0) = 3.48$ T, where the four rf generators were tuned to 47.65, 49.5, 51.03, and 52.95 MHz spanning a bandwidth of 5.3 MHz. These frequencies are clearly visible in the spectrum, which was obtained with a resolution of 1 MHz. At the time of the measurements, 47.15 s, P_{rf} had been ramped from a steady initial 3 MW at 46.9 s to a final 5.6 MW at 47.1 s. The spectrum contains a single, time-delayed MICE line at 40 MHz with narrow width ($\Delta f = 1.4$ MHz) and its second harmonic at 80 MHz. The fact that both single and multifrequency ICRH produce a single down-shifted MICE line shows that this feature is unlikely to be a measurement artifact. This is supported by the observed time delay of the MICE with respect to the switch-on of the ICRH power. The weaker lines seen below 12 MHz are consistent with the beat frequencies among the ICRH and MICE lines. The observation of MICE in discharges with two different magnetic fields (Figs. 2 and 3) allows us to check the field dependence. The ratio of the magnetic fields is 1.35, which is equal to the ratio of the MICE frequencies, within measurement errors of a few percent. We conclude that MICE is fundamentally cyclotronic in nature.

To help identify MICE with specific ions, Fig. 3 shows the radial locations of the cyclotron harmonic resonances of the principal plasma H and D ion species. Frequency matching reveals a correlation between the MICE lines and the minority H resonances at major radius $R = 3.9 \pm 0.1$ m, allowing for the finite resolution of the analyzer.

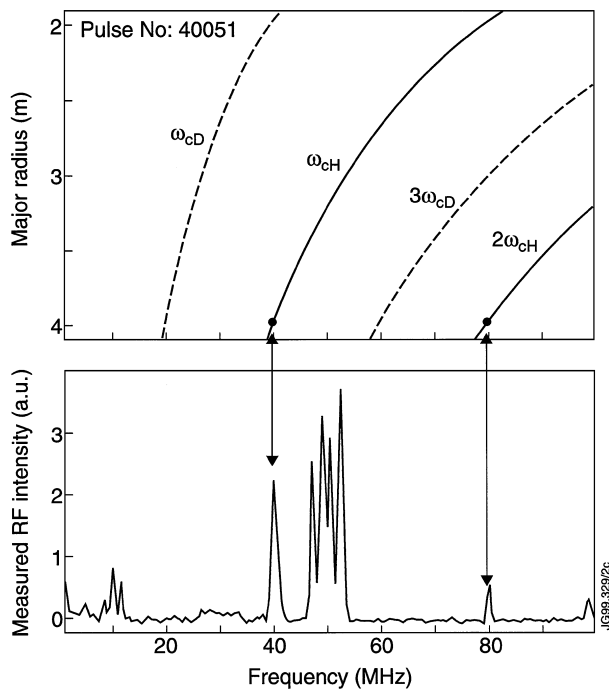


FIG. 3. Lower: rf emission spectra measured during four-frequency ICRH. Fundamental and second harmonic MICE lines are visible at 40 and 80 MHz in this discharge. Upper: Plot of the major radii of the principal plasma H and D ion-cyclotron resonances.

This result confirms the identity of the new emission line as an ion-cyclotron feature associated with H minority ions in the edge plasma. In the plasma midplane, the surface of the ICRH antenna is at radius $R = 3.893$ m; therefore the most probable radial interval for the location of the detected emission source is $3.8 < R < 3.893$ m.

With the spectrum analyzer in single-frequency mode, fast time resolved intensity data at the MICE frequency are seen. In Fig. 4, this was at 29.6 MHz, and data within a 1 MHz bandwidth were collected with sampling rate 0.12 ms. In this discharge, the preprogrammed linear ramp-up of the power started at time 3.6 s and the flat-top level of 4.7 MW reached at time 3.9 s. The MICE intensity data show a delay of approximately 0.4 s after the ICRF flattop before the line switches on at 4.3 s. The rise time for the signal to increase from the noise floor to its maximum level is 1 ms. The appearance of the line is a rapid and not a gradual process. Further changes of signal intensity occur on a similar time scale of 1 ms.

An existence diagram for MICE was constructed from an experimental database of 34 discharges (Fig. 5). The significant parameters were found to be coupled ICRH power, P_{rf} , and total stored fast ion energy in the plasma, W_{fast} , quantities which are coupled [8]. The total anisotropic components of the fast ion energy (associated with ICRH energetic minority ions) is $W_{fast} = \frac{4}{3}(W_{dia} - W_{mhd})$ which was derived experimentally from measurements of total stored diamagnetic

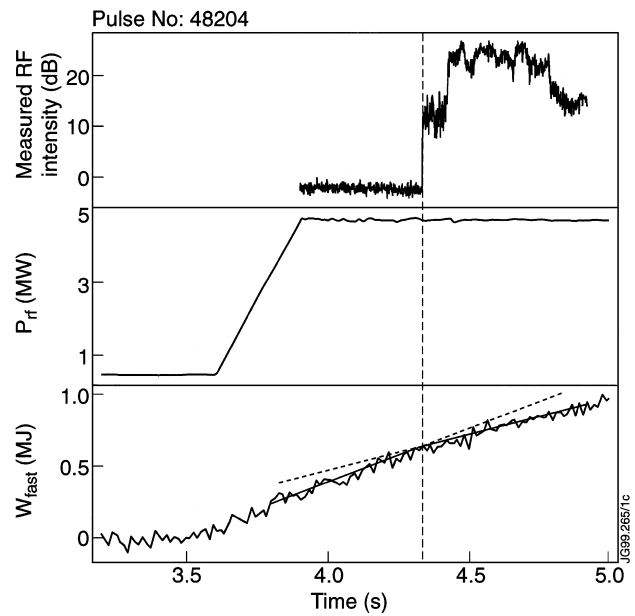


FIG. 4. Upper: Plot of the MICE intensity at 29.6 MHz. The noise floor is at 0 dB. Middle: Trace of the ICRH power coupled to the plasma at 37.3 MHz. Lower: Plot of the total anisotropic component of the plasma stored energy (W_{fast}), associated with ICRH minority ions.

energy, W_{dia} , and total energy in the discharge obtained from equilibrium measurements, W_{mhd} . The errors on W_{fast} are ± 0.3 MJ, represented in Fig. 5 as vertical error bars. The variation of P_{rf} during the measurement time is represented by horizontal bars. Necessary conditions for MICE to be observed are $W_{fast} \geq 0.6$ MJ and $P_{rf} \geq 4.5$ MW.

Figure 4 also shows W_{fast} around the MICE switch-on time. Since energetic minority protons provide the free energy drive for MICE, any correlation between the change in the time derivative $d(W_{fast})/dt$ and the appearance of MICE can be interpreted as an associated power loss,

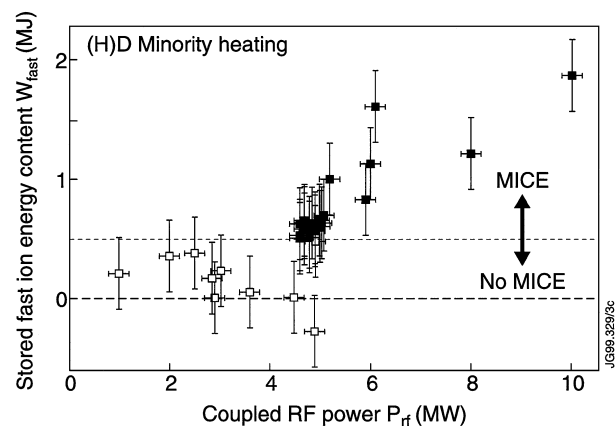


FIG. 5. Existence diagram for MICE constructed from a database of discharges with (H)D ICRF heating displayed in the (W_{fast} , P_{rf}) plane. Filled symbols denote MICE detected; open symbols denote MICE not detected.

ΔP , from the energetic ions. The quantity ΔP gives a measure of all power losses from the minority ions and therefore represents an upper bound on the total radiated MICE power. At the MICE switch-on time, 4.3 s, $\Delta P \approx -0.1 \pm 0.1$ MW, where the negative sign denotes a power loss from minority ions. This loss term constitutes $\approx 2\%$ of P_{rf} . Other loss processes include, for example, the loss of minority ion energy by direct particle interception on outboard limiter surfaces. In fact, during ICRH tokamak operations, camera observations sometimes show the occurrence of local “hot spots” on the plasma-facing surfaces of outboard limiters [11]. The appearance of hot spots is delayed by up to ~ 0.5 s after the ramp-up of P_{rf} , and a possible explanation for the spots is direct interception of ICRH ions on loss orbits. This observation suggests that the same phenomena cause MICE and limiter hot spots.

The properties of MICE may be compared with those of FP-ICE. The two phenomena are similar in that they are both characterized by a localized radiation source in the outer midplane edge of the plasma and are associated with a population of energetic, superthermal ions. It is significant, in this context, that the two sets of measurements were made in JET with antennas located in very different regions of the torus; both the previous FP-ICE and present MICE measurements are consistent with an emission source in this region of the plasma. However, with MICE, there is an observed minimum threshold in W_{fast} or P_{rf} before the emission is observed. This is different in the case of FP-ICE where no threshold in fusion reactivity has thus far been seen. Another important difference is that the frequencies of the MICE lines coincide with harmonics, l , of the H minority gyrofrequency ($\omega = l\Omega_{\text{H}}$), whereas FP-ICE is identified with harmonics of the D and α -particle gyrofrequencies. One of the key observations of MICE is the time delay before it switches on, which is clearly different from FP-ICE where no delay is seen. The delay can be understood in terms of the minority ion rf heating process [7] where resonant minority ions are accelerated from thermal up to high energies before they can participate in MICE. After switch-on of the ICRH, the minority tail evolves on the time scale of τ_s . Typically it takes a time $(1-2)\tau_s$ for the tail to reach near-equilibrium conditions. With the typical JET values given above, the classical expectation is that the minority tail should buildup on a time scale of 0.3–0.6 s, in broad agreement with the observed MICE time delay ~ 0.4 s. For a MICE region of width $\Delta R \sim 0.1$ m and plasma conditions at the MICE threshold, the local concen-

tration of energetic super-Alfvénic protons is of order $n_{\text{H}}/n_e \sim 0.001$. We note that the value of ΔR is close to one orbital Larmor radius (0.11 m) of the 3 MeV proton shown in Fig. 1. Calculations with the ICRH resonance moved to the high field side of the plasma center also show a class of energetic minority ions with sufficiently large orbits to intercept the outer midplane edge plasma. These ions could potentially generate MICE, but no rf measurements have yet been made with this resonance geometry on JET. The geometry of Fig. 1 shows that the excited ICE wave mode, although radially localized, is not strongly poloidally localized.

This paper reports the first measurement of ICE from ICRH minority ions in a tokamak (MICE). These data support the prediction that ICRH particles should generate superthermal MICE although with some differences in behavior compared with FP-ICE which are not fully understood. Theoretical modeling may help resolve the question of the MICE threshold. Future experiments include the use of ^3He minority ions to drive MICE and observing the effect on MICE of scanning the resonance location (thus changing the edge velocity distribution) and the concentration of minority ions (thus changing the average energy of the tail ions).

It is a pleasure to acknowledge the contributions of A. Kaye and A. Franklin in the design and construction of the rf probe and of the many operational staff at JET in the execution of the experiments.

-
- [1] G. A. Cottrell, in *Proceedings of the Course and Workshop on Applications of rf Waves to Tokamak Plasmas, Varenna, 1985* (CEC, Brussels, 1985), Vol. 2, p. 710.
 - [2] G. A. Cottrell *et al.*, in *Proceedings of the 13th European Conference on Controlled Fusion and Plasma Heating, Schliersee, 1986* (European Physical Society, Geneva, 1986), Vol. 10C, Pt. II, p. 37.
 - [3] G. A. Cottrell and R. O. Dendy, *Phys. Rev. Lett.* **60**, 1540 (1988).
 - [4] G. A. Cottrell *et al.*, *Nucl. Fusion* **33**, 1365 (1993).
 - [5] S. R. Cauffman, Ph.D. dissertation, Princeton University, 1997.
 - [6] G. A. Cottrell and D. F. H. Start, *Nucl. Fusion* **31**, 61 (1991).
 - [7] T. H. Stix, *Nucl. Fusion* **15**, 737 (1975).
 - [8] T. E. Stringer, *Plasma Phys.* **16**, 651 (1974).
 - [9] R. O. Dendy *et al.*, *Phys. Plasmas* **1**, 1918 (1994).
 - [10] K. G. McClements *et al.*, *Phys. Rev. Lett.* **82**, 2099 (1999).
 - [11] A. C. C. Sips (private communication).